Published in final edited form as:
Nature. 2004 January 29; 427(6973): 461–465. doi:10.1038/nature02229.

The ADP/ATP translocator is not essential for the mitochondrial permeability transition pore

Jason E. Kokoszka[1,4,*], **Katrina G. Waymire**[1,4], **Shawn E. Levy**[4,*], **James E. Sligh**[4,*], **Jiyang Cai**[5], **Dean P. Jones**[5], **Grant R. MacGregor**[1,2,4], and **Douglas C. Wallace**[1,3,4]

[1]Center for Molecular and Mitochondrial Medicine and Genetics, University of California, Irvine, California 92697, USA

[2]Department of Developmental and Cell Biology, University of California, Irvine, California 92697, USA

[3]Departments of Biological Chemistry and Ecology and Evolutionary Biology, University of California, Irvine, California 92697, USA

[4]Center for Molecular Medicine, Emory University School of Medicine, Atlanta, Georgia 30322, USA

[5]Departments of Medicine and Biochemistry, Emory University School of Medicine, Atlanta, Georgia 30322, USA

Abstract

A sudden increase in permeability of the inner mitochondrial membrane, the so-called mitochondrial permeability transition, is a common feature of apoptosis and is mediated by the mitochondrial permeability transition pore (mtPTP). It is thought that the mtPTP is a protein complex formed by the voltage-dependent anion channel, members of the pro- and anti-apoptotic BAX-BCL2 protein family, cyclophilin D, and the adenine nucleotide (ADP/ATP) translocators (ANTs)[1,2]. The latter exchange mitochondrial ATP for cytosolic ADP and have been implicated in cell death. To investigate the role of the ANTs in the mtPTP, we genetically inactivated the two isoforms of ANT[3–5] in mouse liver and analysed mtPTP activation in isolated mitochondria and the induction of cell death in hepatocytes. Mitochondria lacking ANT could still be induced to undergo permeability transition, resulting in release of cytochrome *c*. However, more Ca^{2+} than usual was required to activate the mtPTP, and the pore could no longer be regulated by ANT ligands. Moreover, hepatocytes without ANT remained competent to respond to various initiators of cell death. Therefore, ANTs are non-essential structural components of the mtPTP, although they do contribute to its regulation.

To investigate the role of ANTs in the mtPTP, we inactivated both the heart-muscle (*Ant1*) and the systemic (*Ant2*) ANT isoform genes in the mouse liver. Humans have three *ANT* genes[6,7], whereas results of complementary DNA library screening[5] and northern and western analyses[3] have suggested that mouse has only two *Ant* genes. To verify this, we screened the Celera and Ensembl mouse genome assemblies, as well as the respective EST

Correspondence and requests for materials should be addressed to D.C.W. (dwallace@uci.edu)..
*Present addresses: Orchid Cellmark, Germantown, Maryland 20874, USA (J.E.K.); Department of Biomedical Informatics (S.E.L.), and Department of Medicine, Dermatology Division (J.E.S.), Vanderbilt University Medical Center, Nashville, Tennessee 37232, USA

Competing interests statement The authors declare competing financial interests: details accompany the paper on www.nature.com/nature.

databases, by BLAST analysis using the *ANT3* cDNA sequence. Consistent with previous results, this produced only two significant matches; that is, *Ant1* and *Ant2*.

Mice with mutations in *Ant1* and *Ant2* were generated by homologous recombination in embryonic stem cells. Mice with a non-conditional null mutant allele of *Ant1* have been described[5]. A CRE-conditional null mutant allele of the X-linked *Ant2* (*Ant2*^{fl}) was produced by generating a targeting vector in which *loxP* sites flanked exons 3 and 4 (Fig. 1a). Targeted embryonic stem cells (Fig. 1b) were used to introduce the conditional floxed allele into the mouse germ line. Liver-specific inactivation of the *Ant2*^{fl} allele was achieved by breeding *Ant2*^{fl} mice with an *Alb-Cre* line of transgenic mice that expresses CRE under control of the liver-specific albumin promoter, which results in the excision of exons 3 and 4 of *Ant2* (Fig. 1a). More than 99% of floxed loci are excised in developing hepatocytes of *Alb-Cre* mice[8]. The *Ant2*^{fl} allele was then bred onto an *Ant1*$^{-/-}$ background[5]. The resulting *Ant1*$^{-/-}$, *Ant2*$^{fl/fl}$ females were crossed with *Ant1*$^{-/-}$, *Ant2*$^{+/Y}$, *Alb-Cre* hemizygous males. Male *Ant1*$^{-/-}$, *Ant2*$^{fl/Y}$, *Alb-Cre* progeny, which are null for both *Ant1* and *Ant2* in their livers, were used to analyse liver mtPTP function. ANT1 is barely detectable in liver[3], and *Ant1*$^{+/+}$, *Ant2*$^{fl/Y}$, *Alb-Cre* animals gave the same results as *Ant1*$^{-/-}$, *Ant2*$^{fl/Y}$, *Alb-Cre* mice (data not shown).

The absence of ANT1 and ANT2 protein in liver mitochondria from *Ant1*$^{-/-}$, *Ant2*$^{fl/Y}$, *Alb-Cre* mice was verified by western blot analysis using isoform-specific antibodies (Fig. 2a). Complete ANT deficiency was confirmed by demonstrating that respiration in mitochondria from *Ant1*$^{-/-}$, *Ant2*$^{fl/Y}$, *Alb-Cre* animals could not be stimulated by the addition of ADP (Fig. 2b). Hence, the liver mitochondria of the *Ant1*$^{-/-}$, *Ant2*$^{fl/Y}$, *Alb-Cre* mice have no ANT.

Endogenous respiration rates of ANT1/ANT2-deficient mitochondria were almost twice that of control mitochondria (34.58 ± 1.6 versus 18.12 ± 1.1 nmol O min^{-1} per mg protein) (Fig. 2b) and the mitochondrial membrane potential ($\Delta P = \Delta\Psi + \Delta pH$) of the ANT-deficient mitochondria was higher than that of controls (191.7 ± 4.9 versus 172.9 ± 3.5 mV). Analysis of the specific activity of OXPHOS enzyme complexes in ANT-deficient mitochondria revealed that complex IV (cytochrome *c* oxidase, COX) was increased more than twofold compared with controls ($P < 0.01$) (Fig. 2c). This was confirmed by western blot analysis, which revealed that the mitochondrial COX subunit I (COI) and cytochrome *c* proteins were more abundant in the ANT-deficient mitochondria (Fig. 2d). Hence, the increased respiration rate is likely to be the result of the specific upregulation in COX activity, suggesting that COX activity may modulate respiration rate. Because ΔP is the product of proton pumping versus proton leak[9], we analysed the level of the systemic uncoupler protein, UCP2, by western blot. UCP2 was downregulated to undetectable levels in the ANT-deficient mitochondria, suggesting that the increased ΔP resulted from decreased proton leak (Fig. 2d).

We then used the ANT-deficient liver mitochondria to investigate the role of ANT in the structure and regulation of the mtPTP. To determine whether the mtPTP was present in the absence of ANT, we isolated mitochondria from livers of ANT-deficient (*Ant1*$^{-/-}$, *Ant2*$^{fl/Y}$, *Alb-Cre*) and ANT-control (*Ant1*$^{-/-}$, *Ant2*$^{fl/Y}$) mice and tested their sensitivity to various inducers of the mtPTP.

Because the mtPTP is a voltage-dependent channel, we determined whether the mtPTP could be activated by the uncoupler carbonyl cyanide *p*-(trifluoromethoxy)phenylhydrazone (FCCP) in the presence of Ca^{2+} (refs [10, 11]) (Fig. 3a, b). Opening of the pore was monitored by mitochondrial swelling through decreased light scattering. Strikingly, ANT-deficient and ANT-control mitochondria responded equally well to FCCP-induced mtPTP activation. To confirm that the mitochondrial swelling was due to the activation of the mtPTP, the

experiment was repeated in the presence of the mtPTP inhibitor cyclosporin A (CsA). This prevented the swelling of both the ANT-control and ANT-deficient mitochondria (Fig. 3a, b). Hence, the ANT-deficient mitochondria have a functional, CsA-inhibitable mtPTP, demonstrating that ANT is not required to form a functional mtPTP.

To further characterize the mtPTP in ANT-deficient mitochondria, we quantified the propensity of ANT-deficient and ANT-control mitochondria to undergo the permeability transition by determining the concentration of Ca^{2+} required to activate the mtPTP and collapse ΔP. Mitochondria were energized with succinate in the presence of the lipophilic cation tetraphenylphosphonium cation (TPP^+). TPP^+ is accumulated into the mitochondrial matrix in proportion to ΔP, and its concentration in the suspension medium can be monitored using a TPP^+-sensitive electrode[12,13]. Aliquots of Ca^{2+} were added to the reaction, each addition causing a transient release of TPP^+ as Ca^{2+} was taken into the mitochondria at the expense of ΔP. The Ca^{2+} additions were repeated until sufficient Ca^{2+} accumulated in the mitochondrial matrix to activate the mtPTP, collapsing ΔP and irreversibly releasing the mitochondrial TPP^+. This process can be inhibited by CsA. Hence, the amount of Ca^{2+} required to cause TPP^+ release provides a quantitative measurement of the sensitivity of the mtPTP.

ANT-deficient liver mitochondria could still be induced to undergo the CsA-inhibitable permeability transition by sequential addition of Ca^{2+} (Fig. 3c). Thus, the existence of a functional mtPTP in the absence of ANT was confirmed. However, threefold more Ca^{2+} was required to activate the mtPTP in the ANT-deficient mitochondria than in the ANT-control mitochondria (Fig. 3c).

Furthermore, in both ANT-deficient and ANT-control mitochondria, activation of the mtPTP (as monitored by Ca^{2+}-induced TPP^+ release—that is, the permeability transition) was associated with the release of cytochrome *c* from the mitochondria into the supernatant. By contrast, the inner membrane COI protein remained associated with the mitochondrial pellets (Fig. 3d). The ANT-deficient mitochondria contained more cytochrome *c* than did controls, so the mutant mitochondria released more cytochrome *c* (Fig. 3d). Hence, ANTs are also not required for mtPTP-induced cytochrome *c* release, confirming that the mtPTP can function in the absence of ANT.

Next, we investigated whether ANTs regulate the function of the mtPTP. ANT-deficient and control liver mitochondria were loaded with TPP^+ and then exposed to various mtPTP effectors. *Tert*-butyl hydroperoxide (*t*-H_2O_2), a non-specific oxidant, and diamide, a specific –SH group oxidant, are both inducers of the mtPTP[14]. These compounds increased the predilection of the mtPTP to undergo the permeability transition, independent of the presence of ANT (Fig. 3e, f). The ANT ligands atractyloside (ATR) and ADP are positive and negative effectors of the mtPTP, respectively[15,16]. Although ATR activated and ADP inhibited the mtPTP in ANT-control mitochondria, they had no effect on ANT-deficient mitochondria (Fig. 3e, f). Thus, the absence of ANT results in the loss of the modulation of the mtPTP by ANT ligands, including adenine nucleotides.

We next investigated whether absence of ANTs affected the response of cultured hepatocytes to inducers of apoptosis and necrosis (Fig. 4). Mitochondrial swelling (Fig. 4a) and cell death (Fig. 4b) occurred in ANT-deficient (*Ant1*$^{-/-}$, *Ant2*$^{fl/Y}$, *Alb-Cre*) hepatocytes after exposure to the calcium ionophore Br-A23187 (ref. [17]). This was partially inhibited by pretreatment with CsA but not with the general caspase inhibitor z-VAD (Fig. 4b). In fact, ANT-deficient hepatocytes were more sensitive to Br-A23187 than were ANT-control cells, suggesting that ANT-deficiency may presensitize the mitochondria to the permeability transition. Moreover, no difference was observed in the sensitivity of ANT-deficient and

ANT-control hepatocytes to treatment with soluble Fas ligand or tumour-necrosis factor-α (TNF-α) in the presence of actinomycin D[18] (Fig. 4c). Hence, ANTs are not required for mitochondrial permeability transition or for these forms of mitochondria-mediated hepatocyte cell death.

In conclusion, our studies reveal that the ANTs are non-essential components of the mtPTP and that they are dispensable for at least some forms of mtPTP-associated cell death. However, the ANTs do have an essential role in regulating permeability transition by modulating the sensitivity of the mtPTP to Ca^{2+} activation and ANT ligands.

Methods

Ant2^{fl} mice on a mixed 129S4 and C57BL/6 background were generated using standard methods under a protocol approved by Emory University's IACUC. The targeting vector contained a floxed *Ant2* gene with a *PGK-neo* cassette added to the 3′-untranslated region (Fig. 1a). Targeted AK7.1 embryonic stem cell clones were identified by Southern analysis (Fig. 1b). The 5′-probe (probe A) detected a 12.8-kilobase (kb) *Xba I* fragment for the wild-type *Ant2* allele and a 6.6-kb fragment for the targeted allele. The 3′-probe (probe B) detected a 7.9-kb *Dra III* fragment for the wild-type allele and a 13.8-kb fragment for the targeted allele. Site-specific recombination between the *loxP* sites removed the last third of the ANT2 coding sequence, including putative transmembrane domains 5 and 6, plus the *PGK-neo* cassette, generating a non-functional protein.

Ant2 was genotyped by PCR (forward primer 5′-ACTCAACCTAGGGCCTTGTG-3′, reverse primer 5′-GGGAGCATTCCTGAAAAATAA-3′; 35 cycles at 94 °C for 20 s; at 56 °C for 30 s; at 72 °C for 40 s) to detect the targeted (485 base pairs, bp) and wild-type (384 bp) alleles. The mutant *Ant2* allele (850 bp) was detected using the same forward primer and reverse primer 5′-GACTTACCCTCCACGACAGC-3′; 35 cycles at 94 °C for 20 s; at 65 °C for 30 s; at 72 °C for 60 s. Genotyping at *Ant1* was determined as described[5].

For western blots, isoform-specific ANT1 and ANT2 antibodies[5], and antibodies recognizing COI, UCP2 and cytochrome c (Molecular Probes and Zymed) were employed. These were reacted to isolated mitochondrial protein (20 μg) or supernatants separated by SDS–PAGE and blotted onto nitrocellulose.

Mitochondria were isolated from liver by homogenization followed by differential centrifugation. Respiration and OXPHOS enzyme activities were normalized for protein concentration using the Coomassie Stain kit (Pierce)[13,19]. Mitochondrial membrane potential was calculated from mitochondrial uptake of TPP^+ using a TPP^+-sensitive electrode . The sensitivity of the mtPTP to undergo permeability transition was examined in liver mitochondria of 10-month-old *Ant1*$^{-/-}$, *Ant2*$^{fl/Y}$, *Alb-Cre* animals by TPP^+ release after sequential additions of 10 nM $CaCl_2$ (ref. [13]). The mtPTP modulators used were 1 mM *t*-H_2O_2, 0.1 mM diamide, 100 μM ATR and 125 μM ADP (Fig. 3).

Mitochondrial PTP activation was also monitored by mitochondrial swelling using light scattering at 546 nm for 10 min in 1.5 ml with 1 mg mitochondrial protein and 16.5 nmol $CaCl_2$. The reaction was initiated by the addition of 0.1 μM ruthenium red and 1 μM FCCP.

Hepatocytes were isolated from 12- to 15-month-old anaesthetized mice, perfused *in situ* with collagenase-dispase medium (Invitrogen). Hepatocytes were gently released, filtered and cultured on collagen-coated cover glasses or plates in Waymouth's MB-752/1 medium[17]. Hepatocyte sensitivity to Ca^{2+} ionophore was examined by extent of cell death assessed by the percentage of total cellular lactate dehydrogenase (LDH) released into the medium[20] after treatment with 5 to 50 μM Br-A23187 for 1 h, without or with a 30 min

pretreatment of either 1 μM CsA or 50 μM z-VAD 17 (Fig. 4). Receptor-induced cell death was monitored by analysis of nuclear morphology using Hoechst 33258 (Molecular Probes) staining after treatment with 100 ng ml^{-1} of murine recombinant TNF-α (R&D Systems) or 4 ng ml^{-1} of human recombinant Fas ligand (Upstate), with or without 0.2 μg ml^{-1} actinomycin D (Fig. 4).

Acknowledgments

We thank M. Magnuson for providing the *Alb-Cre* transgenic mice, L. Hayes for mouse husbandry and genotyping, and H. Yi for the electron microscope analysis. This work was funded by US National Institutes of Health grants awarded to D.C.W., G.R.M. and D.P.J.

References

1. Zoratti M, Szabo I. The mitochondrial permeability transition. Biochim. Biophys. Acta 1995;1241:139–176. [PubMed: 7640294]
2. Marzo I, et al. Bax and adenine nucleotide translocator cooperate in the mitochondrial control of apoptosis. Science 1998;281:2027–2031. [PubMed: 9748162]
3. Levy SE, Chen Y-S, Graham BH, Wallace DC. Expression and sequence analysis of the mouse adenine nucleotide translocase 1 and 2 genes. Gene 2000;254:57–66. [PubMed: 10974536]
4. Ellison JW, Salido EC, Shapiro LJ. Genetic mapping of the adenine nucleotide translocase-2 gene (Ant2) to the mouse proximal X chromosome. Genomics 1996;36:369–371. [PubMed: 8812469]
5. Graham B, et al. A mouse model for mitochondrial myopathy and cardiomyopathy resulting from a deficiency in the heart/skeletal muscle isoform of the adenine nucleotide translocator. Nature Genet 1997;16:226–234. [PubMed: 9207786]
6. Stepien G, Torroni A, Chung AB, Hodge JA, Wallace DC. Differential expression of adenine nucleotide translocator isoforms in mammalian tissues and during muscle cell differentiation. J. Biol. Chem 1992;267:14592–14597. [PubMed: 1378836]
7. Lunardi J, Hurko O, Engel WK, Attardi G. The multiple ADP/ATP translocase genes are differentially expressed during human muscle development. J. Biol. Chem 1992;267:15267–15270. [PubMed: 1639771]
8. Postic C, Magnuson MA. DNA excision in liver by an albumin-Cre transgene occurs progressively with age. Genesis 2000;26:149–150. [PubMed: 10686614]
9. Boss O, Hagen T, Lowell BB. Uncoupling proteins 2 and 3: potential regulators of mitochondrial energy metabolism. Diabetes 2000;49:143–156. [PubMed: 10868929]
10. Petronilli V, Nicolli A, Costantini P, Colonna R, Bernardi P. Regulation of the permeability transition pore, a voltage-dependent mitochondrial channel inhibited by cyclosporin A. Biochim. Biophys. Acta 1994;1187:255–259. [PubMed: 7521212]
11. Bernardi P. Modulation of the mitochondrial cyclosporin A-sensitive permeability transition pore by the proton electrochemical gradient. Evidence that the pore can be opened by membrane depolarization. J. Biol. Chem 1992;267:8834–8839. [PubMed: 1374381]
12. Esposito LA, et al. Mitochondrial oxidative stress in mice lacking the glutathione peroxidase-1 gene. Free Radic. Biol. Med 2000;28:754–766. [PubMed: 10754271]
13. Kokoszka JE, Coskun P, Esposito L, Wallace DC. Increased mitochondrial oxidative stress in the Sod2 mouse results in the age-related decline of mitochondrial function culminating in increased apoptosis. Proc. Natl Acad. Sci. USA 2001;98:2278–2283. [PubMed: 11226230]
14. Halestrap AP, Woodfield KY, Connern CP. Oxidative stress, thiol reagents, and membrane potential modulate the mitochondrial permeability transition by affecting nucleotide binding to the adenine nucleotide translocase. J. Biol. Chem 1997;272:3346–3354. [PubMed: 9013575]
15. Lapidus RG, Sokolove PM. The mitochondrial permeability transition. Interactions of spermine, ADP, and inorganic phosphate. J. Biol. Chem 1994;269:18931–18936. [PubMed: 8034650]
16. Novgorodov SA, Gudz TI, Brierley GP, Pfeiffer DR. Magnesium ion modulates the sensitivity of the mitochondrial permeability transition pore to cyclosporin A and ADP. Arch. Biochem. Biophys 1994;311:219–228. [PubMed: 8203884]

17. Qian T, Herman B, Lemasters JJ. The mitochondrial permeability transition mediates both necrotic and apoptotic death of hepatocytes exposed to Br-A23187. Toxicol. Appl. Pharmacol 1999;154:117–125. [PubMed: 9925795]

18. Hatano E, et al. The mitochondrial permeability transition augments Fas-induced apoptosis in mouse hepatocytes. J. Biol. Chem 2000;275:11814–11823. [PubMed: 10766806]

19. Trounce IA, Kim YL, Jun AS, Wallace DC. Assessment of mitochondrial oxidative phosphorylation in patient muscle biopsies, lymphoblasts, and transmitochondrial cell lines. Methods Enzymol 1996;264:484–509. [PubMed: 8965721]

20. Leist M, et al. Murine hepatocyte apoptosis induced in vitro and in vivo by TNF-α requires transcriptional arrest. J. Immunol 1994;153:1778–1788. [PubMed: 8046244]

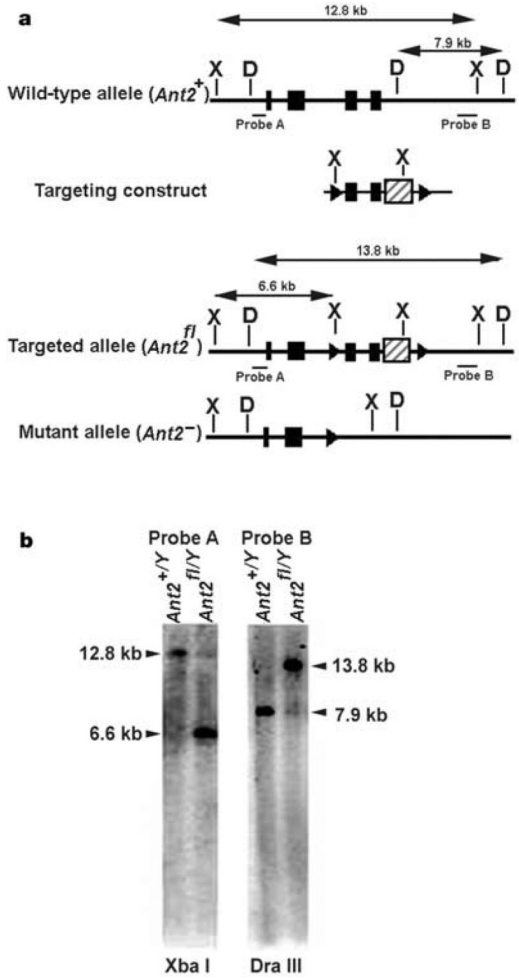

Figure 1.

Preparation of a CRE-conditional *Ant2*-null mutant allele in mouse embryonic stem cells. **a**, Top to bottom, maps of the wild-type *Ant2* locus, the region of homology within the targeting construct, and the floxed ($Ant2^{fl}$) and mutant ($Ant2^{-}$) alleles. Exons (black boxes), *loxP* sites flanking exons 3 and 4 (triangles), *PGKneo* selection cassette within 3′UTR (hatched box). **a**, **b**, Arrows indicate sizes of Xba I (X) and Dra III (D) restriction fragments used to identify correctly targeted clones by Southern analysis of embryonic-stem-cell genomic DNA using probes A and B. **b**, Southern blot of targeted and untargeted embryonic-stem-cell clones.

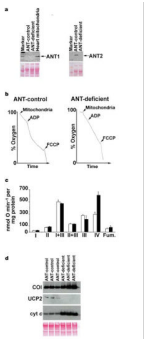

Figure 2.

Inactivation of ANT in liver mitochondria. **a**, Western blots of mitochondria using ANT1 and ANT2-specific antibodies. Heart mitochondria are a positive ANT1 control. ANT1 and ANT2 are both 30 kDa (arrows). The Ponceau-S-stained blot (below) is the loading control. **b**, ADP-stimulated mitochondrial respiration. Arrowheads denote addition of 600 μg of mitochondrial protein, 125 nmol of ADP and 75 nM FCCP. **c**, OXPHOS enzyme activities of ANT-control (white bars) or ANT-deficient (black bars) liver mitochondria (mean of three mice each). OXPHOS complexes I–IV and fumarase (Fum.) are shown. Error bars show the standard error. **d**, Western blots of mitochondria from three independent mice for COI (56 kDa), UCP2 (33 kDa), cytochrome (cyt) *c* (11 kDa). The Ponceau S blot (below) is the loading control.

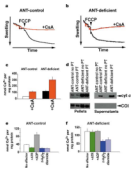

Figure 3.

Effect of ANT-deficiency on mtPTP activation in liver mitochondria. **a**, ANT-control and **b**, ANT-deficient mtPTP activation by Δ*P* depolarization (FCCP) monitored by mitochondrial swelling. Black trace, no CsA; red trace, with CsA. **c**, Amount of Ca^{2+} required per mg of mitochondrial protein to activate the mtPTP and collapse Δ*P*. **d**, Western blots of cytochrome *c* released into the supernatant fraction versus COI retained in the mitochondrial pellet following Ca^{2+}-activation of the mtPTP. **e**, ANT-control and **f**, ANT-deficient Ca^{2+}-activation of the mtPTP in the presence of positive and negative effectors.

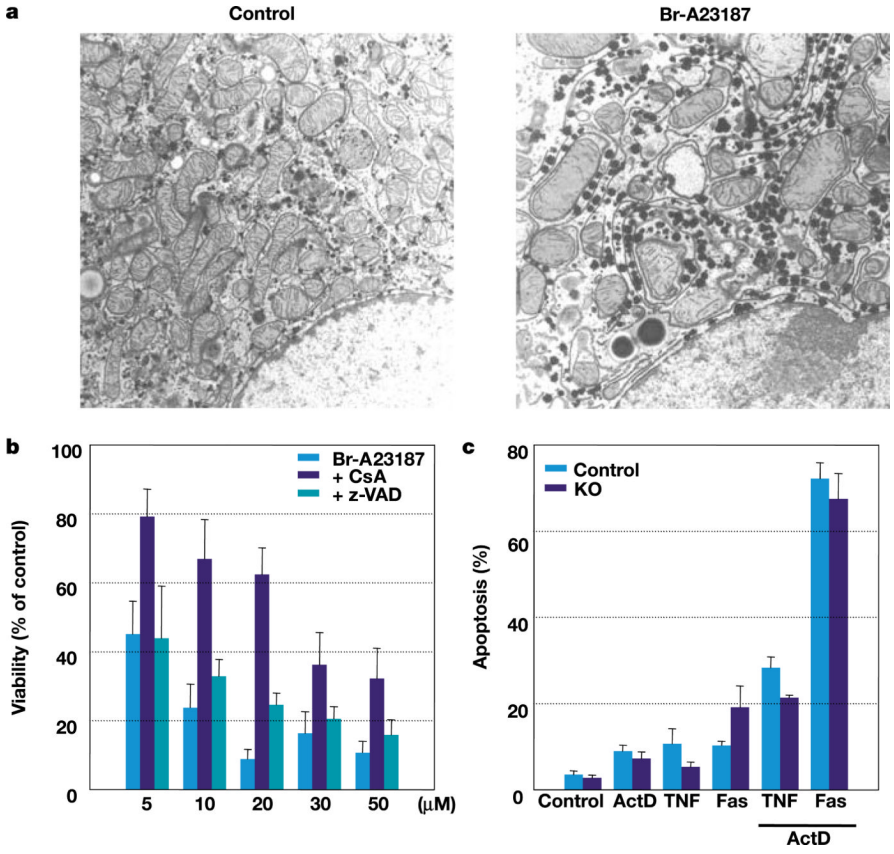

Figure 4.

Induction of cell death in ANT-deficient mouse hepatocytes. **a**, Transmission electron microscope images of ANT-deficient hepatocytes. Control, untreated; Br-A23187, treated for 1 h with 10 μM Br-A23187. **b**, Calcium ionophore (Br-A23187) induced cell death (% of LDH released) of ANT-deficient treated hepatocytes relative to untreated hepatocytes, without or with pretreatment by either CsA or z-VAD. **c**, Receptor-mediated apoptosis (Hoechst 33258 analysed nuclear fragmentation) induced by TNF-α or soluble Fas ligand treatment, with or without actinomycin D (ActD). KO, knockout.